New developments in fracture of rubbers: Predictive tools and influence of thermal aging

Moussa Naït-Abdelaziz, Georges Ayoub, Xavier Colin, M. Benhassine, M. Mouwakeh

New developments in fracture of rubbers: Predictive tools and influence of thermal aging

M. Nait Abdelaziz[a,*], G. Ayoub[b,*], X. Colin[c], M. Benhassine[d], M. Mouwakeh[e]

[a] Université de Lille, UML EA 7512, Unité de Mécanique de Lille, 59000 Lille, France
[b] Department of Industrial and Manufacturing Systems Engineering, University of Michigan-Dearborn, Dearborn, MI 48128 USA
[c] Laboratoire des Procédés et Ingénierie en Mécanique et Matériaux (PIMM), UMR CNRS 8006, Arts et Métiers ParisTech, 151 boulevard de l'Hôpital, F-75013 Paris, France
[d] Département MMC, EDF Lab, avenue des Renardières, F-77818 Moret-sur-Loing, France
[e] Department of Applied Mechanics, Faculty of Mech. Eng., Aleppo University, Aleppo, Syria

Keywords:
Rubber
Thermal aging
Post-crosslinking
Continuum damage mechanics
Energy limiter approach
Ultimate mechanical properties

A B S T R A C T

In this work, the influence of thermal oxidative aging on the ultimate mechanical properties of rubbers is investigated. Two new approaches to predict failure properties are proposed. The first one is the stress limiter approach that uses a "damage" parameter allowing determination of the failure stress and strain of an aged material knowing both the mechanical properties and macromolecular network characteristics of an as-received material. The second one is an extension of the energy limiter approach that suggests capturing the drop of the stress at failure by replacing the strain energy density function of an as-received elastomeric material by a function expressed in terms of an energy limiter. The predictive capabilities of these two approaches are validated using experimental results for two elastomeric materials: an EPDM and a polychloroprene (CR), both of which exhibit a largely predominant post-crosslinking (over chain scissions) during aging. Comparison between the predictions and the experimental results in terms of failure stresses and strains under uniaxial tension showed a good agreement. Consequently, these two approaches are promising tools for designing elastomeric parts subjected to thermal oxidative aging.

1. Introduction

The extremely high ductility with very low strength and the high damping and insulating properties of elastomeric materials are suitable for a wide range of industrial applications, such as in electrical insulation, medical devices, and air and ground transportation. Elastomeric materials are subjected to extreme loading conditions, such as complex mechanical loadings, high temperatures, UV radiations, oxygen and humidity. Consequently, their mechanical and ultimate properties are influenced by the operating conditions. Therefore, the development of models capturing the alteration in those properties is essential for guiding the design of elastomeric material components. The mechanical and ultimate properties of elastomers are strongly dependent on the loading condition history and on the chemical and physical aging exposure history. Those properties are directly influenced by the changes in the macromolecular network structure induced by a chemical reaction (i.e. oxidation but also hydrolysis) (Colclough et al., 1968; Dunn and Scanlan, 1961; Mullins, 1956; Tobolsky et al., 1950; Yu and Wall, 1965).

Since the middle of the last century, several research investigations have focused on elucidating the thermal aging mechanisms of elastomeric materials that directly affect their mechanical properties. It is reported that thermal oxidation progressively alters the chemical composition of elastomeric materials (consumption and depletion of the weakest C–H bonds, formation and accumulation of a wide variety of oxidation products, etc.), which consequently modifies their macromolecular network structure (Belbachir et al., 2010; Ben Hassine et al., 2014; Clavreul, 1997; Colin et al., 2007a,b,c; Delor-Jestin, 1996; Gillen et al., 2006; Ha-Anh and Vu-Khanh, 2005; Rivaton et al., 2005; Shabani, 2013; Tomer et al., 2007). The alteration in the macromolecular network structure induced by thermal oxidation is the result of two main competitive mechanisms: post-crosslinking and chain scissions. Their relative predominance depends on both the chemical composition of the elastomer and the thermal aging exposure conditions. For instance, the chain scission mechanism is found to be predominant in peroxide-vulcanized NR and EPDM rubbers

* Corresponding authors.
E-mail addresses: Moussa.Nait-Abdelaziz@univ-lille.fr (M. Nait Abdelaziz), gayoub@umich.edu (G. Ayoub).

(Delor-Jestin, 1996; Shabani, 2013), whereas post-crosslinking is largely favored when they are vulcanized with sulfur due to maturation phenomena (Ben Hassine et al., 2014; Delor-Jestin, 1996). However, maturation can be totally supplanted by reversion phenomena when increasing the temperature (Bevilacqua, 1962; Colin et al., 2007b; Shelton, 1957). Post-crosslinking leads to the formation of new cross-link nodes and thus to the reduction of the average molar mass between two consecutive cross-links of the network. In contrast, chain scissions destroy the elastic active chains and thus lead to the formation of dangling chains, but without changing the average molar mass between two consecutive cross-link nodes (Azura and Thomas, 2006; White and Shyichuk, 2007). Remarkably, the ultimate mechanical properties are independent of the involved network alteration mechanism. It was reported that the ultimate properties of elastomers decrease with increasing aging time; however, stiffness and yielding increase when post-crosslinking is predominant and decrease when chain scissions prevail (Celina et al., 2005; Cristiano et al., 2011; Le Gac et al., 2016, 2014; Mark and Tang, 1984; Neuhaus et al., 2017; Pourmand et al., 2017; Rivaton et al., 2005). Investigating the thermal aging effects on the mechanical, physical and chemical properties of polymers requires thorough knowledge in the field of chemical-physical analytical techniques and in the field of mechanical testing (Celina et al., 2005; Clavreul, 1997; Colin et al., 2007b).

The prediction of the long-term behavior of rubbers in severe environmental conditions requires the establishment of non-empirical behavior laws taking into account the structural changes at lower scales, especially at the macromolecular one. At this scale, the pertinent structural variables would be the concentration of cross-link nodes or the average molar mass between two consecutive cross-links if post-crosslinking is predominant, or the concentration chain scissions or dangling chains if chain scissions prevail. However, the validity of these predictive tools can be checked only if reliable experimental data are available, although concerns are raised on the reliability of the accelerated aging processes (Gillen et al., 2005).

Many authors have applied the time-temperature equivalence principle, based on the Arrhenius relationship, on both mechanical, physical and chemical properties to study accelerated thermal aging of polymers (Gillen et al., 2003; Rivaton et al., 2005; Scheirs et al., 1995; Wise et al., 1995; Woo et al., 2010). The time-temperature equivalence principle is used to extrapolate material performance under soft aging conditions from experimental data obtained under accelerated thermal aging conditions performed at elevated temperatures. The development of the time-temperature equivalence principle correlates with viscoelastic polymers' mechanical behavior evolution with increasing strain rate or decreasing temperature. A shift factor a_T is used to superimpose the evolution of the investigated materials or mechanical properties as a function of aging conditions for the purpose of building a master curve (Ferry, 1980; Treloar, 1971a,b). In particular for thermal aging, the investigated material's property is plotted versus the aging condition (exposure time) for different temperatures. The shift factor a_T will be applied to superimpose all the data and determine the master curve at a reference temperature. The master curve can be tentatively used to estimate the investigated parameters at lower temperatures and longer exposure time, which are often inaccessible during a conventional research study. Two expressions of the shift factor can be generally used:

The first one is based upon an Arrhenius-type law, which takes the following form:

$$\ln(a_T) = -\frac{E_a}{R}\left(\frac{1}{T} - \frac{1}{T_0}\right) \tag{1}$$

where E_a is the activation energy, T is the absolute temperature, T_0 is the reference temperature, and R is the perfect gas constant.

The pertinence of this approach for studying polymer aging was established by many authors (Ben Hassine et al., 2014; Gillen et al., 2006; Ha-Anh and Vu-Khanh, 2005; Wise et al., 1995). However, the Arrhenius-based shift factor a_T is generally used for temperatures above the polymer glass transition temperature T_g, typically when $T_0 > T_g + 100$.

If the studied aging process temperatures do not fall within the reference temperature restriction, it becomes more relevant to use the approach suggested by Williams et al. (1955), known as the WLF approach. In this case, the shift factor is expressed according to the following equation:

$$\ln(a_T) = \frac{C_1(T - T_0)}{C_2 + T - T_0} \tag{2}$$

C_1 and C_2 are material-dependent parameters to be determined by fitting the experimental data obtained at a given reference temperature T_0 with Eq. (2).

From a mechanical point of view, many attempts were made in this last decade to develop fracture criteria for rubbers. For example, Dal and Kaliske (2009) proposed a micro-mechanical model consisting, at a micro-scale, of a serial construction of a Langevin-type spring (to capture the entropic elasticity) and a bond potential representing the interatomic bond energy acting in the chain. To achieve the micro-macro scale transition, the authors used a micro-sphere model (Miehe et al., 2004) and a numerical integration scheme. The approach was successfully used for the prediction of fracture in rubbers under biaxial loading and for oxidized rubbers. The only drawback is that the approach requires a numerical implementation in a finite element (FE) code to be exploited.

Another interesting approach was developed by Volokh (2016, 2017, 2010, 2007). The energy limiter concept was introduced in order to limit the stored energy in the rubber when subjected to mechanical loading. Indeed, the classical hyperelastic constitutive laws do not capture the stress drop resulting from the material fracture. By introducing the energy limiter, it is therefore possible to describe the entire curve, including the stress drop. The main features of this approach are summarized later in this paper.

In recent investigations, Naït-Abdelaziz et al. (2012) and Ben Hassine et al. (2014) proposed an original approach based on the intrinsic defect concept to describe the fracture behavior of elastomers under biaxial loadings and also to predict the ultimate stresses and strains when thermo-oxidative aging is involved.

More generally, approaches using continuum damage mechanics, following the pioneering work of Kachanov (1980) and Lemaitre (1985), were successfully proposed to predict elastomeric materials failure under fatigue loading (Ayoub et al., 2014, 2012, 2011). In this sense, the energy limiter approach (Volokh, 2010) can be considered as a continuum damage approach since the material's softening under mechanical loading is considered.

The research focuses of this work are two: first is developing a stress limiter parameter for predicting the aging effects on stresses and strains at break for rubbers. The second focus is extending the energy limiter approach to investigate fracture of thermally aged elastomers by developing a fracture criterion.

2. Ultimate properties predictors

Two different approaches are presented in this section, the stress limiter and the extended energy limiter approaches. We start by presenting the theoretical equations describing the mechanical behavior of rubbers.

The macromolecular network of rubbers consists of randomly oriented interlinked long chains. The deformation of rubbers is associated with the decrease of the macromolecular network entropy induced by the alignment of the macromolecular chains along the loading direction. Rubbers exhibit a highly nonlinear stress–strain

behavior usually described as visco-hyperelastic behavior (Treloar, 1971a,b). The mechanical behavior of elastomers is described in the literature with either physically based approaches (based on statistical theories) (Arruda and Boyce, 1993; James and Guth, 1943; Treloar, 1971) or phenomenological approaches (based on invariant continuum mechanics theory) (Ogden, 1997; Rivlin, 1948; Yeoh, 1990). In this paper, the Neo-Hookean model, a physically based approach proposed by Treloar (1971a,b), is used. This approach uses a statistical Gaussian model to describe the kinematics of a single macromolecular chain. The strain energy density W of a perfect network may be written as follows:

$$W = \frac{\rho RT}{2M_c}\left(\lambda_1^2 + \lambda_2^2 + \lambda_3^2 - 3\right) \tag{3}$$

where ρ the volumetric mass, T is the absolute temperature, R is the gas constant, and M_c is the average molar mass between two consecutive cross-links of the network and λ_i represents the principal stretches (i.e. the principal components of the strain gradient tensor).

To account for the mobility of the junction nodes, James and Guth (1943) modified the Neo-Hookean model and derived the so-called phantom network model, written as follows:

$$W = \frac{\rho RT}{2M_c}\left(1 - \frac{2}{f}\right)\left(\lambda_1^2 + \lambda_2^2 + \lambda_3^2 - 3\right) \tag{4}$$

where f is the crosslink functionality (i.e., the number of elastically active chains connected to the same crosslink node).

The principal Cauchy stresses σ_i may be derived as follows:

$$\sigma_i = \lambda_i \frac{\partial W}{\partial \lambda_i} - p \tag{5}$$

The boundary conditions of a specific loading case are used to determine the hydrostatic pressure p. In the case of uniaxial tension, this leads to:

$$\sigma = \frac{\rho RT}{M_c}\left(1 - \frac{2}{f}\right)\left(\lambda^2 - \frac{1}{\lambda}\right) \tag{6}$$

where σ and λ are the true stress and the stretch in the loading direction, respectively. The thermal aging, which acts on the molar mass, can be accounted for in the model by introducing an appropriate evolution kinetics in Eq. (6). Indeed, stiffening as well as softening can be captured by the molar mass evolution depending on the predominant mechanism: post-crosslinking (molar mass decreases and the stiffness increases) or chain scission (inverse effect). In analogy with damage mechanics, a "damage" parameter can be expressed as a function of the molar mass since the latter is associated with the variation of the material's stiffness.

2.1. Stress limiter definition

In this section, the mathematical framework of the proposed stress limiter approach is presented. The modified Neo-Hookean approach Eq. (6) does not depict the behavior of the rubber in the fracture regime and therefore its validity is limited to the range of stress values below the stress at break σ_b:

$$\sigma \leq \sigma_b \tag{7}$$

And therefore the stress at break can be written as follows:

$$\sigma_b = \frac{\rho RT}{M_c}\left(1 - \frac{2}{f}\right).\left(\lambda_b^2 - \frac{1}{\lambda_b}\right) \tag{8}$$

As mentioned previously, the thermal degradation of rubber is accompanied with a reduction of the average molar mass M_c, which results into a reduction in the materials ductility. The ratio of stresses at break for the as-received σ_{b_0} and thermally aged σ_b materials can be written as follows:

$$\frac{\sigma_b}{\sigma_{b_0}} = \frac{M_{c_0}\left(\lambda_b^2 - \frac{1}{\lambda_b}\right)}{M_c\left(\lambda_{b_0}^2 - \frac{1}{\lambda_{b_0}}\right)} \tag{9}$$

where suffix 0 refers to the as-received material and suffix b denotes the value at break. In analogy with damage mechanics theory, the stress at break can be written alternatively as follows:

$$\sigma_b = \sigma_{b_0}(1 - D) \tag{10}$$

the factor $(1-D)$ is a stress limiter that depends on the molar mass between two consecutive crosslinks of the network. We will start by assuming that the stress limiter can be expressed as follows, which will be also experimentally proved:

$$(1 - D) = \frac{M_c - M_{c_y}}{M_{c_0} - M_{c_y}} = \mu_R \tag{11}$$

where μ_R is the reduced molar mass. The limit conditions are satisfied by Eq. (11) as noted:

$$\begin{cases} \sigma_b = \sigma_{b_0} \; if \; M_c = M_{c_0} \\ \sigma_b = 0 \; if \; M_c = M_{c_y} \end{cases} \tag{12}$$

where M_{c_y} is a yield molar mass value below which the material is fully degraded. Note that more elaborate expressions of the stress limiter factor could be obtained when combining Eqs. (9) and (10):

$$1 - D = \frac{M_{c_0}\left(\lambda_b^2 - \frac{1}{\lambda_b}\right)}{M_c\left(\lambda_{b_0}^2 - \frac{1}{\lambda_{b_0}}\right)} \tag{13}$$

An explicit expression of the stress limiter can be obtained by using the perfect network theory. The complete mechanical response, including beyond-fracture behavior, can be described by modifying slightly Eq. (6) as follows:

$$\sigma = \frac{\rho RT}{M_c}\left(1 - \frac{2}{f}\right).\left(\lambda^2 - \frac{1}{\lambda}\right)F(M_c) \tag{14}$$

where $F(M_c)$ is a modified sigmoid (s-shaped) function verifying the following conditions:

$$\begin{cases} F = 1 \; if \; \lambda < \lambda_b \\ F \to 0 \; if \; \lambda \geq \lambda_b \end{cases} \tag{15}$$

And $F(M_c)$ is expressed as follows:

$$F(x(\lambda, M_c)) = \frac{e^{-\left(\frac{x}{a}\right)}}{1 + e^{-\left(\frac{x}{a}\right)}} \tag{16}$$

where a is a parameter controlling the slope of the drop and x is a molar mass and stretch dependent function. The expression of x is deduced by combining Eqs. (11) and (13):

$$x(\lambda, M_c) = \left(\lambda^2 - \lambda^{-1}\right) - \left(\frac{M_c}{M_{c_0}}\right).\left(\frac{M_c - M_{c_y}}{M_{c_0} - M_{c_y}}\right).\left(\lambda_{b_0}^2 - \lambda_{b_0}^{-1}\right) \tag{17}$$

Note that the input parameters are M_{c_0}, M_{c_y} and λ_{b_0}. It is worth noting that the proposed Eqs. (10) and (11) enable the prediction of the stress values at break for a given thermal aging state while the derived Eq. (14) enable the description of the entire stress–strain mechanical response up to complete fracture.

2.2. Extended energy limiter approach

In this section, we start by summarizing the theoretical framework of the energy limiter approach introduced by Volokh (2007). Volokh originally proposed capturing the drop of the stress at failure by replacing the strain energy density function W of an as-received elastomeric material by a function $\psi(W)$ expressed in

terms of an energy limiter ϕ. As a first attempt, the following function was proposed by the author:

$$\psi(W) = \phi - \phi e^{-W/\phi} \tag{18}$$

The expression of the Cauchy stress tensor as derived by Volokh (2007) is as follows:

$$\overline{\overline{\sigma}} = 2J^{-1}\overline{\overline{F}}\frac{\partial W}{\partial \overline{\overline{C}}}\overline{\overline{F}}^{T} e^{-W/\phi} \tag{19}$$

where J is the determinant of the deformation gradient tensor $\overline{\overline{F}}$, and $\overline{\overline{C}}$ is the right Cauchy –Green strain tensor. The exponential term contributes to progressively decrease the stress and consequently to soften the material behavior up to complete failure. Nevertheless, with such an expression, the sharpness of the stress drop at failure cannot be captured (indeed, rubber sheets generally fail in a "brittle" manner). Hence, an updated energy potential expression was proposed (Volokh, 2010):

$$\psi(W) = \frac{\phi}{m}\left[\Gamma\left(\frac{1}{m}, 0\right) - \Gamma\left(\frac{1}{m}, \frac{W^m}{\phi^m}\right)\right] \tag{20}$$

where Γ is the upper gamma function defined as:

$$\Gamma(s,\xi) = \int_{\xi}^{\infty} t^{s-1}e^{-t}dt \tag{21}$$

Knowing that $\partial\Gamma(s,x)/\partial x = -x^{s-1}e^{-x}$, the Cauchy stress tensor was derived as:

$$\overline{\overline{\sigma}} = 2J^{-1}\overline{\overline{F}}\frac{\partial W}{\partial \overline{\overline{C}}}\overline{\overline{F}}^{T} e^{\left(-\frac{W^m}{\phi^m}\right)} \tag{22}$$

The input parameter m allows to control the sharpness of the drop. It is worth noting that using the energy limiter described in Eq. (20) must be restricted to monotonic loading as the behavior induced by this potential is reversible. In Volokh (2014), the author extended this approach to capture the irreversibility induced by fracture. Nevertheless, in our study, we attempt to demonstrate the capability of the approach to capture the evolution of the stress at break with aging. Therefore, it is necessary to include the irreversibility of fracture as suggested by Volokh (2014), when extending the approach to multiaxial/structural loadings.

In what follows, the energy limiter is developed for uniaxial tension. For this specific loading condition, the stress tensor is reduced to only one non-zero value, i.e., the stress in the loading direction, while, under the incompressibility assumption, the deformation gradient is expressed as:

$$[F] = \begin{bmatrix} \lambda & 0 & 0 \\ 0 & 1/\sqrt{\lambda} & 0 \\ 0 & 0 & 1/\sqrt{\lambda} \end{bmatrix} \tag{23}$$

with λ being the stretch in the loading direction. The strain energy density expressed in Eq. (4) is used to calculate the stress in Eq. (22):

$$\sigma = \frac{\rho RT}{M_c}\left(1 - \frac{2}{f}\right)\left(\lambda^2 - \frac{1}{\lambda}\right)e^{\left(-\frac{W^m}{\phi^m}\right)} \tag{24}$$

Eq. (24) allows the description of the complete stress–strain response in uniaxial tension. Note that the stress at break is $\sigma_b = \max[\sigma]$. In what follow, we propose to modify the expression of the energy limiter to account for the degradation of the mechanical properties induced by aging. We can postulate, as a first attempt, that the energy limiter is a function of the molar mass between crosslinks and assume linear evolution from a maximum value ϕ_0 associated with the as-received material, as follows:

$$\phi(M_c) = \frac{M_c - M_{c_y}}{M_{c_0} - M_{c_y}}\phi_0 \tag{25}$$

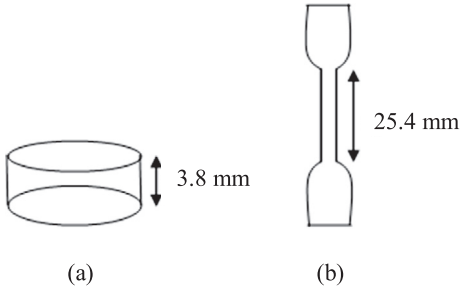

Fig. 1. Specimen geometries for: (a) average molar mass measurements, (b) tensile tests.

Note that the parameters of Eq. (25) are the same as those defined previously in Eq. (11) except for ϕ_0, which must be identified from a tensile test on a as-received material.

A non-linear evolution can also be introduced by slightly modifying Eq. (25) as follows:

$$\phi(M_c) = \left(\frac{M_c - M_{c_y}}{M_{c_0} - M_{c_y}}\right)^{\alpha}\phi_0 \tag{26}$$

an additional parameter α needs to be identified. In the next section, the experimental results used for the validation of the two newly proposed approaches are reported.

3. Experimental material and procedure

3.1. Materials

Two materials are considered in this work: EPDM and CR. EPDM is an ethylene-propylene-diene monomer rubber vulcanized by 4 phr of sulfur compounds in the presence of activators (ZnO and acid stearic) and accelerators (TMTD and MBTS) and filled by 13 and 29.8 wt% of carbon black and clay platelets, respectively. It is noteworthy that the EPDM gum has been carefully characterized by FTIR spectrometry and ^{1}H NMR before vulcanization. It was found that the repetitive and constitutive unit of the polymer chain is composed of 66.1 mol% ethylene, 33.1 mol% propylene, and 0.8 mol% norbornene (ENB).

CR is a polychloroprene rubber also vulcanized with sulfur compounds, whose exact chemical composition and thermal aging behavior were reported by Le Gac et al. (2014).

3.2. Specimens

For the EPDM rubber, two different specimen geometries (Fig. 1) are used in this work: the first one (flat discs) to measure the average molar mass evolution M_c between two consecutive cross-links of the network by using a swelling technique, the second one (dog-bone specimens) to get the strain-stress response up to failure. All of these specimens are cut from rubber sheets of 3.8 mm thickness.

For the CR rubber, Le Gac et al. (2014) used dogbone specimens of type 2 (from ISO 37) cut from rubber sheets of 0.9 mm thickness.

3.3. Accelerated thermal aging

For the EPDM rubber, the accelerated aging process consists of exposing the two specimen types to 130, 150, and 170 °C in air-ventilated ovens for various lengths of time. During the exposure, the dog-bone specimens were kept in a vertical position using a specifically designed apparatus in order to avoid any shape change at high temperature.

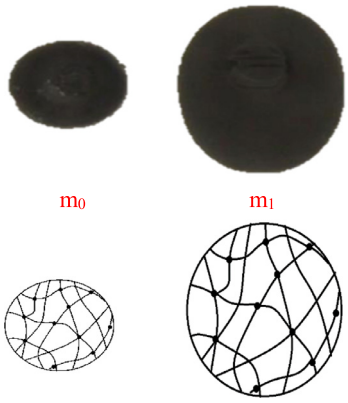

Fig. 2. EPDM specimen before and after swelling for molar mass measurements.

For each temperature and exposure-time aging condition, the type two specimens were swelled at room temperature (25 °C) with cyclohexane. This operation induces a network volume expansion, as shown in Fig. 2.

According to the literature, the average molar mass between crosslinks M_c is determined from the volume change using the classical Flory–Rehner's relationship. For a 4-functional network, the average molar mass between two consecutive crosslinks M_c is expressed as follows (Flory and Rehner, 1943; Flory, 19537):

$$M_c = -\frac{0.5V\rho_p\left(V_{r0}^{1/3} - 0.5V_{r0}\right)}{\ln(1-V_{r0}) + V_{r0} + \chi V_{r0}^2} \tag{27}$$

where V is the molar volume of solvent (cm^3/mol), ρ_p is the EPDM density equal to 0.86 g/cm^3, χ is the Flory–Huggins' interaction parameter equal to 0.321 for the EPDM-cyclohexane system (Baldwin and Ver Strate, 1972; Hilborn and Ranaby, 1989), and V_{r0} is the polymer volume fraction in the swollen network expressed as:

$$V_{r0} = \frac{\rho_{solvent}}{\rho_{solvent} + (m_g/m_s - 1)\rho_{polymer}} \tag{28}$$

Where m_g is the weight of the swollen polymer sample, m_s is the weight of the same sample after drying under vacuum at 40 °C for 24 h, and $\rho_{solvent}$ is the solvent density (0.78 g/cm^3 for cyclohexane).

For the CR rubber, thermal aging was performed in air-ventilated ovens at several temperatures ranging from 60 to 140 °C. More details are given by the authors in reference (Le Gac et al., 2014).

3.4. Uniaxial tension tests

The stress–strain mechanical response and the fracture properties of the EPDM rubber are determined under monotonic uniaxial tension tests. Tests are conducted at room temperature (25 °C) under a constant crosshead speed of 5 mm/min. The local strains are measured using a non-contact videosystem that tracks the displacement of two spots pre-printed on the specimen.

A crosshead speed of 10 mm/min is used to characterize the mechanical and fracture behavior of the CR rubber, and the strains are calculated from the crosshead displacement (Le Gac et al., 2014).

4. Model results and discussions

In this section, we will start by presenting the evolution of the average molar mass M_c as a function of the thermal aging conditions. Indeed, the evolution of M_c with thermal aging is an input for both proposed models, the stress limiter and the energy limiter concepts. The WLF theory is used to determine the master curve of the evolution of M_c with thermal aging. In section one, the predictive capability of the stress limiter approach is presented, while in section two the prediction results of the energy limiter approach are presented.

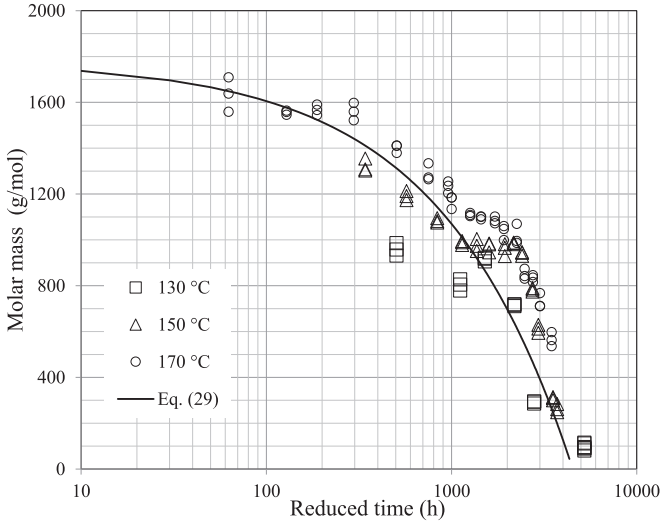

Fig. 3. Molar mass as a function of the reduced time (logarithmic scale) for EPDM material.

4.1. Molar mass evolution

The average molar mass of the thermally aged and as-received EPDM material was determined using the swelling method described in Section 3.3. The time-temperature equivalence Eq. (2) is used to find the master curve of the M_c evolution. Fig. 3 shows the evolution of the molar mass as a function of the reduced time $= t^* a_T$ with t being the exposure-time and a_T is determined using the WLF approach in Eq. (2). The optimized WLF parameters are the following: $T_0 = 403$ K, $C_1 = -70$, and $C_2 = 900$ K. The resulting master curve can be fitted using the following expression:

$$M_c = M_{c_0} - ae^{b\ln t_r} \tag{29}$$

with M_{c0}= 1780 g/mole, $a = 14$, and $b = 0.55$.

For the CR rubber, only one aging temperature is provided by the authors (Le Gac et al., 2014), the temperature of accelerated aging being 100 °C. Fig. 4 shows the evolution of the molar mass as a function of the reduced aging time. The experimental data evolution can be fitted using Eq. (29), with the following parameters: M_{c0}= 10,500 g/mole, $a = 2500$, and $b = 0.2$. Note that the average molar mass is not measured experimentally but estimated by fitting Eq. (6) on the experimental stress–strain data and by assuming that the functionality factor is equal to $f = 4$.

4.2. Stress limiter approach results and discussions

In this section, the predictive capability of the stress limiter approach is analyzed by comparing the numerical results to the thermal aging experimental results of the EPDM rubber.

As introduced in Eq. (10), the ratio between the stresses at break of the thermally aged and as-received materials (also referred to as reduced stress) is expressed as follows:

$$(1-D) = \frac{\sigma_b}{\sigma_{b_0}} = \Sigma_R \tag{30}$$

In section two, it is assumed that this ratio depends on the average molar mass (Eq. (11)). The validity of this assumption is checked by plotting the evolution of the reduced stress Σ_R as a

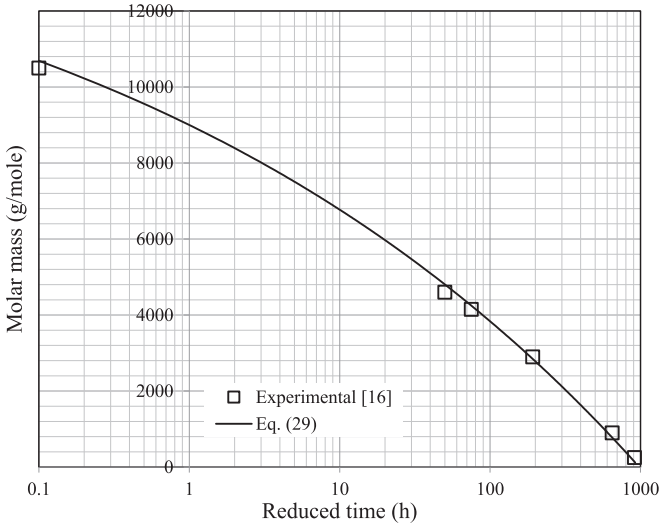

Fig. 4. Molar mass as a function of reduced aging time for CR rubber.

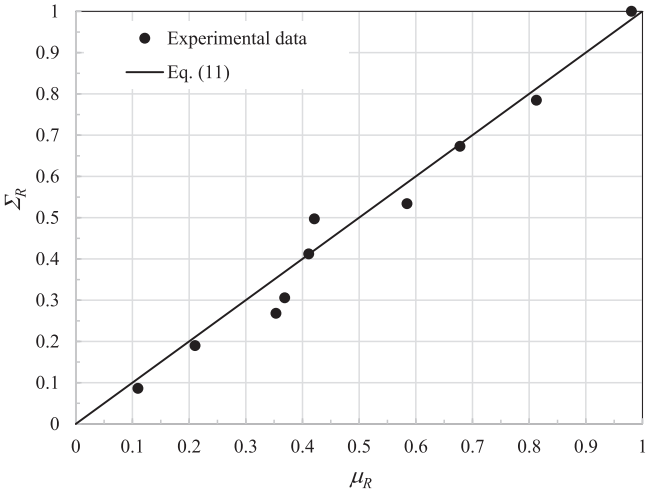

Fig. 5. Evolution of the reduced stress as a function of the reduced molar mass. (aged EPDM, 170 °C).

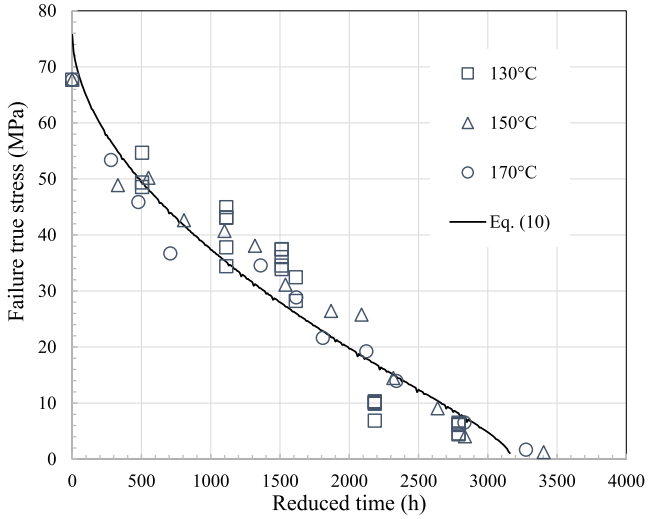

Fig. 6. Stress at break as a function of reduced time of aging.

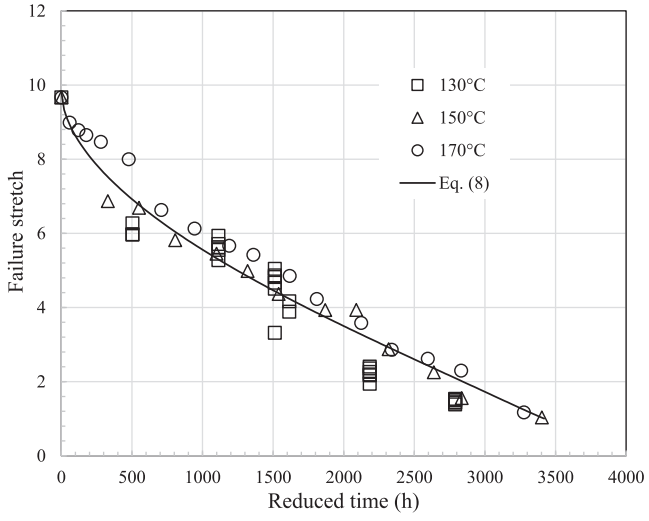

Fig. 7. Stretch at break as a function of reduced time of aging.

function of the reduced molar mass μ_R for the EPDM material aged at a temperature of 170 °C, as illustrated in Fig. 5. The reduced molar mass μ_R was determined by using the following parameters: $M_{c_y} = 600$g/mol and $M_{c_0} = 1780$g/mol. Fig. 5 shows a linear relationship between the Σ_R and the μ_R. Furthermore, it is clearly highlighted that $\mu_R = \Sigma_R$, which proves the validity of Eq. (11). This finding proves that the decrease of the stress at break with thermal aging can be directly related to the change of average molecular mass M_c. Therefore, the assumptions of the stress limiter approach are valid and allow the prediction of the stress at break for thermally aged EPDM.

The stress at break for the different thermally aged samples (or for a reduced time) can be determined from Eq. (10) by knowing the average molar mass and the stress at break of the as-received material. Fig. 6 shows the evolution of the stress at break as a function of the reduced time of aging for all EPDM thermal aging experiments. The stress to break calculated using the stress limiter approach exhibits a trend with tight scattering around the prediction of Eq. (10), resulting from using the WLF theory for the calculation of the reduced time. The evolution of the stress at break shows a quick decrease for low "reduced time," followed by a linear decrease with increasing "reduced time." This evolution is in correlation with the evolution trend exhibited by the average molar mass M_c with increasing "reduced time." In fact, the decrease of the stress at break with increasing "reduced time" is the result of chains reaching their limit of extensibility at an earlier deformation stage, which results from the decrease in the average number of monomers between crosslinks. The implementation of the proposed approach is relatively simple and is summarized by Eqs. (2) and (10). However, this theory requires the evolution of the molar mass (determined in Eq. (29)) as imputed and two additional experimentally determined parameters: the yield average molar mass M_{c_y} and the stress at break for the as-received material.

In what follows, to further confirm the relevance of the stress limiter approach, the evolution of the stretches at break λ_b is analyzed. The stretch at break for each thermal aging experiment is calculated using Eq. (8), which uses the stress at break as an input. The stretches at break λ_b are obtained by numerically solving a nonlinear equation (Eq. (8)) using Newton's method.

Fig. 7 shows the evolution of the stretch at break for different aging conditions (reduced time). The experimental results exhibit tight scattered points around the model prediction (Eq. (8)). A quick decrease for low "reduced time" in the stretch to break is observed, followed by a linear decrease with increasing "reduced time." Obviously, the evolution of the stretch to break follows the

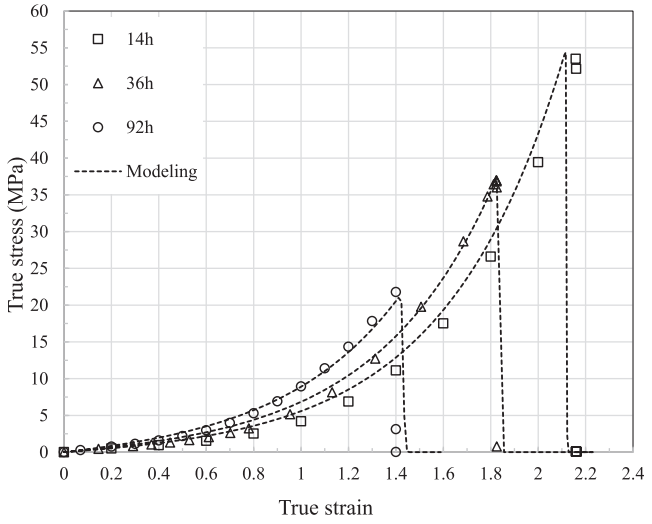

Fig. 8. Cauchy stress as a function of true strain (dots: experimental, lines: Eq. (14)).

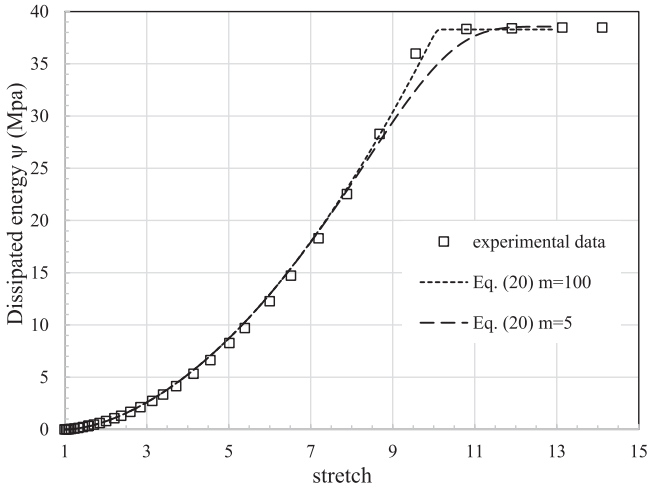

Fig. 9. Dissipated energy as a function of true strain for the as received EPDM material.

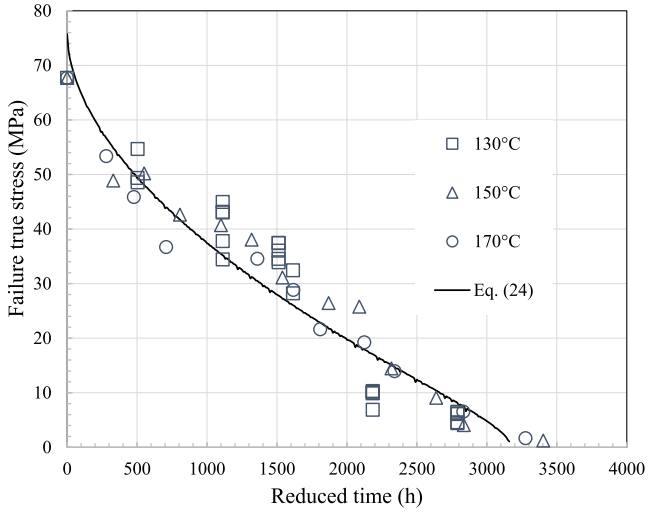

Fig. 10. Stress at break as a function of reduced time of aging.

observed and predicted evolutions of the average molar mass M_c and the stress to break, respectively. The decrease in the stretch to break with increasing "reduced time" is the direct consequence of chains reaching their limit of extensibility as the average number of monomers between crosslinks is decreasing. In a simplified way, as the length of the molecular chains is decreasing, they can be stretched less. The good agreement between the experimental and the predicted evolutions evidences the applicability of this approach to predict the behavior of thermo-oxidative aged elastomeric materials.

The stress–strain behavior of EPDM samples aged at 170 °C for 3 exposure times is presented in Fig. 8. An increase in the hardening (the rubbery modulus) and a decrease in the strain to break and stress to break with increasing aging time are observed in Fig. 8. While we are presenting only the 170 °C results, the other temperatures exhibit similar trends. The evolution of the stress–strain response of thermally aged EPDM is described by Eq. (14). Fig. 8 also shows a comparison between the experimental and the predicted stress–strain response of thermally aged EPDM samples at 170 °C and for 14-, 36-, and 96-hour exposure times. The predictive capabilities of the model are clearly highlighted. The model is capable of accurately mimicking the increase of the hardening (rubbery modulus). Furthermore, the model is able to predict accurately the stresses and strains at break. This approach is considered a simplified approach, as the complete behavior including break can be accounted for, and therefore it becomes an attractive tool for designing elastomeric parts subjected to thermo-oxidative aging.

4.3. Energy limiter approach

4.3.1. Energy limiter approach applied to EPDM rubber

In this section, the energy limiter approach predictions are compared to the EPDM and CR thermal aging experiments. As already mentioned, the energy limiter allows the dissipated energy to be bound at its maximum value reached at failure.

Fig. 9 presents a comparison between the experimental and the energy limiter approach predicted dissipated energy evolution as a function of the true strain for as-received EPDM material. The relevance of this approach is highlighted by the close fit between the energy limiter approach and the experiments. The experimental dissipated energy is obtained by calculating the area under the true stress–strain curve, while the theoretical one is estimated by using Eq. (20). The strain energy density W is calculated using Eq. (4). The value of the energy limiter is found to be equal to $\phi = \phi_0 = 38.5\ MPa$ for $m = 100$, and it slightly depends on the value of m. Note that changing the value of the parameter m helps in controlling the shape of the transition to failure. The calculation of the upper gamma function is achieved using Matlab software. This figure allows identification of the parameter ϕ_0. In what follows, the parameter m is chosen to be equal to 100.

The evolution of the energy limiter during thermal aging is calculated using the evolution law presented by Eq. (25), with the evolution parameters taken to be equal to $M_{c_y} = 600$g/mol and $\phi_0 = 38.5$MPa, where ϕ_0 is the as-received energy limiter and M_{c_y} is the yield average molar mass. The values of the stress at break can be computed as a function of the average molar mass of the thermally aged sample by evaluating the maximum value of the stress given by Eq. (24). The obtained data can, therefore, be plotted as a function of the reduced time using the WLF principle and Eq. (29).

Fig. 10 shows the comparison between the experimental results and the estimates given by the energy limiter approach of the stress at break for the different thermal aging conditions. The good agreement between the experimental and predicted data confirms the relevance of this approach in studying thermal aging.

Moreover, the correctness of using the energy limiter approach to predict the mechanical properties of thermally aged EPDM is

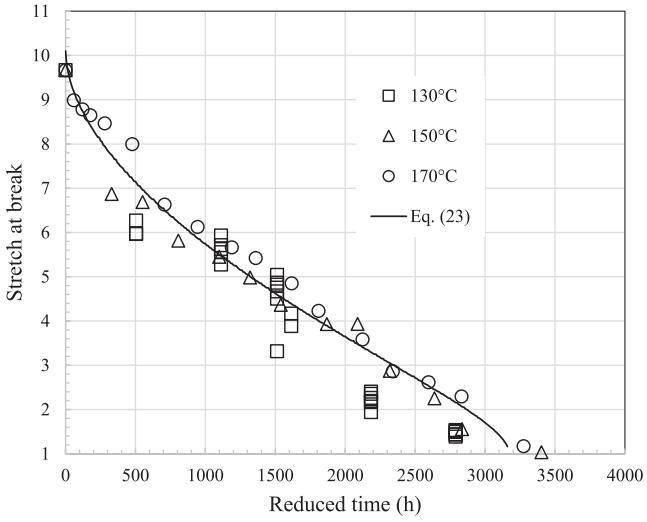

Fig. 11. Stretch at break as a function of reduced time of aging.

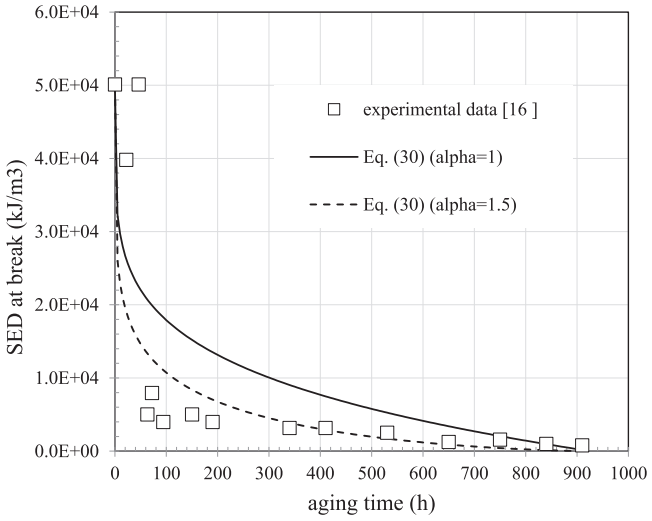

Fig. 12. Failure energy density as a function of time of aging, ϕ is expressed using Eq. (26).

clearly confirmed when comparing the experimental stretches at break to the estimated ones, where again a good agreement is found, as shown in Fig. 11.

Furthermore, a similarity is noticed between the predictions of the stress limiter approach and the energy limiter approach. Indeed, both approaches mimic the evolutions of the stress and stretch at break with evolving thermal aging conditions. The stress and stretch at break decrease non-linearly at low levels of "reduced time," and a linear decrease is observed with increasing "reduced time." However, the energy limiter approach, in general, predicts a slightly earlier fracture than the stress limiter approach.

4.3.2. Energy limiter approach applied to CR rubber

As previously mentioned, the data presented by Le Gac et al. (2014) are used to validate the energy limiter approach. The authors provided the evolution of the dissipated energy density and of the strain at break as a function of the aging time (only one temperature was investigated). The molar mass between crosslinks was indirectly calculated by fitting the experimental stress-strain curves according to Eq. (6). The evolution of the molar mass as a function of the "reduced time" is presented in Fig. 4.

The predicted dissipated energy is computed by using Eq. (20). Moreover, the energy at break is obtained by extracting the maximum value of the predicted dissipated energy:

$$\psi_{failure} = \max\left[\psi(W)\right] = \frac{\phi}{m}\left[\Gamma\left(\frac{1}{m}, 0\right)\right] \tag{31}$$

The model parameters used in this calculation are the following: $M_{c_y} = 700\text{g/mol}$, $M_{c_0} = 10,500\text{g/mol}$, $\phi_0 = 50\text{MPa}$ and $m = 100$. The stretch at break is then deduced from Eq. (24) by using a Newton algorithm. Figs. 12 and 13 present the evolution of the energy and stretch at break as a function of the aging time. It is observed that the energy approach predictions overestimate the experimental data (it corresponds to the plots with alpha being equal to 1 which is equivalent to Eq. (25)). It is proposed to improve the prediction capability of the energy approach by using the non-linear form given in Eq. (26). A value of the exponent α of 5 is found to present the best predictions of the studied CR experimental data.

From both Figs. 12 and 13 we can observe that the ultimate properties drastically decrease in the early period of aging. This rapid decrease is attributed to the fact that no anti-oxidant additive is used in the manufacturing process of the CR rubber. Furthermore, the induced crystallization exhibited by CR rubbers makes

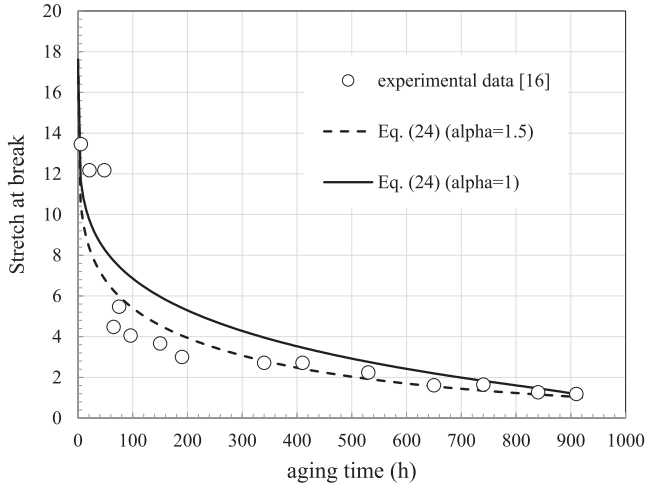

Fig. 13. Stretch at break as a function of time of aging, ϕ is expressed using Eq. (26).

their fracture behavior more complex than that of amorphous rubbers such as EPDM. Indeed, as reported by Le Gac et al. (2014), strain-induced crystallization highly improves the fracture properties of the as-received material. Nevertheless, oxidative crosslinking induced by thermal aging diminishes the influence of induced recrystallization on the mechanical behavior, and it rapidly vanishes after very short exposure times.

5. Conclusion

In this work, two new approaches are proposed to estimate the ultimate mechanical properties of elastomeric materials subjected to thermal oxidative aging.

The first approach, the stress limiter approach, is based upon an analogy with continuum damage mechanics, in which a damage parameter is formulated in order to predict the stress at break of thermally aged elastomeric materials, knowing the as-received material properties. It is found that for materials exhibiting post-crosslinking induced thermal aging damage, the best description of the degradation behavior is obtained when the damage parameter is expressed as a function of the average molar mass between crosslinks. Based on the comparison between the experimental and prediction results on EPDM rubber, a linear variation of the

damage parameter is capable of giving good estimates of the ultimate stresses and stretches. This approach also allows prediction of the complete mechanical behavior of the material in terms of strain-stress response beyond the failure. Although the model predictions mimic the experimental results, this approach is developed only for uniaxial tension, and an effort must be made to generalize the formulation to account for multiaxial loading paths, including non-proportional loadings.

To address this issue, an extension of the energy limiter approach developed initially by Volokh (2016, 2017, 2010, 2007) is proposed. Similar to the stress limiter approach, the energy limiter parameter is written as a function of the average molar mass between crosslinks. As a first approximation, a linear evolution is proposed, therefore reducing the number of parameters to be identified. A very good agreement is found between the EPDM rubber experimental data and the prediction. However, to better predict the experimental data of the CR rubber, it is necessary to use a non-linear evolution of ϕ.

The advantage of the energy limiter approach is its ability to investigate complex loadings since it is based upon a thermodynamic formulation, which allows tonsorial stresses and strains to be derived. Finally, the damage parameter chosen in this investigation is directly linked to the molar mass between two consecutive crosslinks. It is therefore important to go further by investigating materials that exhibit chain scission and check the capabilities of these approaches to be generalized.

References

Arruda, E.M., Boyce, M.C., 1993. A three-dimensional constitutive model for the large stretch behavior of rubber elastic materials. J. Mech. Phys. Solids 41, 389–412. https://doi.org/http://dx.doi.org/10.1016/0022-5096(93)90013-6.

Ayoub, G., Naït-Abdelaziz, M., Zaïri, F., 2014. Multiaxial fatigue life predictors for rubbers: application of recent developments to a carbon-filled SBR. Int. J. Fatigue 66.. https://doi.org/10.1016/j.ijfatigue.2014.03.026.

Ayoub, G., Naït-Abdelaziz, M., Zaïri, F., Gloaguen, J.M., Charrier, P., 2012. Fatigue life prediction of rubber-like materials under multiaxial loading using a continuum damage mechanics approach: effects of two-blocks loading and R ratio. Mech. Mater. 52. https://doi.org/10.1016/j.mechmat.2012.03.012.

Ayoub, G., Naït-Abdelaziz, M., Zaïri, F., Gloaguen, J.M., Charrier, P., 2011. A continuum damage model for the high-cycle fatigue life prediction of styrene-butadiene rubber under multiaxial loading. Int. J. Solids Struct. 48. https://doi.org/10.1016/j.ijsolstr.20104.003.

Azura, A.R., Thomas, A.G., 2006. Effect of heat ageing on crosslinking, scission and mechanical properties. In: Elastomers and Components: Service Life Prediction – Progress and Challenges, pp. 27–38. https://doi.org/10.1533/9781845691134.

Baldwin, F.P., Ver Strate, G., 1972. Polyolefin elastomers based on ethylene and propylene. Rubber Chem. Technol. 45, 709–788.

Belbachir, S., Zaïri, F., Ayoub, G., Maschke, U., Naït-Abdelaziz, M., Gloaguen, J.M., Benguediab, M., Lefebvre, J.M., 2010. Modelling of photodegradation effect on elastic-viscoplastic behaviour of amorphous polylactic acid films. J. Mech. Phys. Solids 58. https://doi.org/10.1016/j.jmps.2009.10.003.

Ben Hassine, M., Naït-Abdelaziz, M., Zaïri, F., Colin, X., Tourcher, C., Marque, G., 2014. Time to failure prediction in rubber components subjected to thermal ageing: a combined approach based upon the intrinsic defect concept and the fracture mechanics. Mech. Mater. 79, 15–24. https://doi.org/10.1016/j.mechmat.2014.07.015.

Bevilacqua, E.M., 1962. Autooxidation and antioxidants. In: Lundberg, W.O. (Ed.), Autooxidation and Antioxidants. New York, pp. 857–918.

Celina, M., Gillen, K.T., Assink, R.A., 2005. Accelerated aging and lifetime prediction: review of non-Arrhenius behaviour due to two competing processes. Polym. Degrad. Stab.. https://doi.org/10.1016/j.polymdegradstab.2005.05.004.

Clavreul, R., 1997. Evolution of ethylene propylene copolymers properties during ageing. Nucl. Instrum. Methods Phys. Res. Sect. B Beam Interact. Mater. Atoms 131, 192–197. https://doi.org/10.1016/S0168-583X(97)00139-0.

Colclough, T., Cunneen, J.I., Higgins, G.M.C., 1968. Oxidative aging of natural rubber vulcanizates. Part III. Crosslink scission in monosulfidic networks. J. Appl. Polym. Sci. 12, 295–307. https://doi.org/10.1002/app.1968.070120205.

Colin, X., Audouin, L., Verdu, J., 2007a. Kinetic modelling of the thermal oxidation of polyisoprene elastomers. Part 3: oxidation induced changes of elastic properties. Polym. Degrad. Stab. 92, 906–914. https://doi.org/10.1016/j.polymdegradstab.2007.0013.

Colin, X., Audouin, L., Verdu, J., 2007b. Kinetic modelling of the thermal oxidation of polyisoprene elastomers. Part 1: unvulcanized unstabilized polyisoprene. Polym. Degrad. Stab. 92, 886–897. https://doi.org/10.1016/j.polymdegradstab.2007.0017.

Colin, X., Audouin, L., Verdu, J., Le Huy, M., 2007c. Kinetic modelling of the thermal oxidation of polyisoprene elastomers. Part 2: effect of sulfur vulcanization on mass changes and thickness distribution of oxidation products during thermal oxidation. Polym. Degrad. Stab. 92, 898–905. https://doi.org/10.1016/j.polymdegradstab.2007.0004.

Cristiano, A., Marcellan, A., Keestra, B.J., Steeman, P., Creton, C., 2011. Fracture of model polyurethane elastomeric networks. J. Polym. Sci. Part B Polym. Phys. 49, 355–367. https://doi.org/10.1002/polb.22186.

Dal, H., Kaliske, M., 2009. A micro-continuum-mechanical material model for failure of rubber-like materials: application to ageing-induced fracturing. J. Mech. Phys. Solids 57, 1340–1356. https://doi.org/10.1016/j.jmps.2009.04.007.

Delor-Jestin, F., 1996. Long Term Thermal and Photochemical Behavior of Elastomers For Applications in the Automotive Field. Blaise Pascal, Clermont-Ferrand, France.

Dunn, J.R., Scanlan, J., 1961. Changes in the stress–strain properties of natural rubber vulcanizates during ageing. Trans. Faraday Soc. 57, 160. https://doi.org/10.1039/tf9615700160.

Ferry, J.D., 1980. Viscoelastic properties of polymers, Viscoelastic viscoelastic properties of polymers.

Flory, P.J., Rehner, J., 1943. Statistical mechanics of crosslinked polymer networks II. Swelling. J. Chem. Phys. 11 (11), 521–526. http://dx.doi.org/10.1063/1723792.

Flory, P.J., 1953. Principles of Polymer Chemistry. Cornell University Press, Ithaca.

Gillen, K.T., Bernstein, R., Celina, M., 2005. Non-Arrhenius behavior for oxidative degradation of chlorosulfonated polyethylene materials. Polym. Degrad. Stab. 87, 335–346. https://doi.org/10.1016/j.polymdegradstab.2004.09.004.

Gillen, K.T., Bernstein, R., Clough, R.L., Celina, M., 2006. Lifetime predictions for semi-crystalline cable insulation materials: I. Mechanical properties and oxygen consumption measurements on EPR materials. Polym. Degrad. Stab. 91, 2146–2156. https://doi.org/10.1016/j.polymdegradstab.2006.0009.

Gillen, K.T., Celina, M., Bernstein, R., 2003. Validation of improved methods for predicting long-term elastomeric seal lifetimes from compression stress-relaxation and oxygen consumption techniques. Polym. Degrad. Stab. 82, 25–35. https://doi.org/10.1016/S0141-3910(03)00159-9.

Ha-Anh, T., Vu-Khanh, T., 2005. Prediction of mechanical properties of polychloroprene during thermo-oxidative aging. Polym. Test. 24, 775–780. https://doi.org/10.1016/j.polymertesting.2005.03.016.

Hilborn, J., Ranaby, B., 1989. Photocrosslinking of EPDM elastomers. Photocrosslinkable compositions. Rubber Chem. Technol. 62, 592–608.

James, H.M., Guth, E., 1943. Theory of the elastic properties of rubber. J. Chem. Phys. 11. 455–48 https://doi.org/10.1063/1723785.

Kachanov, M.L., 1980. Continuum model of medium with cracks. J. Eng. Mech. Div. 106 (5), 1039–1051.

Le Gac, P.Y., Broudin, M., Roux, G., Verdu, J., Davies, P., Fayolle, B., 2014. Role of strain induced crystallization and oxidative crosslinking in fracture properties of rubbers. Polymer 55 (10), 2535–2542. https://doi.org/10.1016/j.polymer.2014.03.023.

Le Gac, P.Y., Celina, M., Roux, G., Verdu, J., Davies, P., Fayolle, B., 2016. Predictive ageing of elastomers: oxidation driven modulus changes for polychloroprene. Polym. Degrad. Stab. 130, 348–355. https://doi.org/10.1016/j.polymdegradstab.2016.06.014.

Lemaitre, J., 1985. A continuous damage mechanics model for ductile fracture. J. Eng. Mater. Technol. 107, 83–89. https://doi.org/10.1115/3225775.

Mark, J.E., Tang, M.Y., 1984. Dependence of the elastomeric properties of bimodal networks on the lengths and amounts of the short chains. J. Polym. Sci. Polym. Phys. 22, 1849–1855.

Miehe, C., Göktepe, S., Lulei, F., 2004. A micro-macro approach to rubber-like materials – Part I: the non-affine micro-sphere model of rubber elasticity. J. Mech. Phys. Solids 52, 2617–2660. https://doi.org/10.1016/j.jmps.2004.03.011.

Mullins, L., 1956. Determination of degree of crosslinking in natural rubber vulcanizates. Part I. J. Polym. Sci. 19, 225–236. https://doi.org/10.1002/pol.1956.120199201.

Naït-Abdelaziz, M., Zaïri, F., Qu, Z., Hamdi, A., Aït Hocine, N., 2012. J integral as a fracture criterion of rubber-like materials using the intrinsic defect concept. Mech. Mater. 53, 80–90. https://doi.org/10.1016/j.mechmat.2012.05.001.

Neuhaus, C., Lion, A., Johlitz, M., Heuler, P., Barkhoff, M., Duisen, F., 2017. Fatigue behaviour of an elastomer under consideration of ageing effects. Int. J. Fatigue 104, 72–80. https://doi.org/10.1016/j.ijfatigue.2017.07.010.

Ogden, R.W.W., 1997. Non-Linear Elastic Deformations Engineering Analysis https://doi.org/10.1016/0955-7997(84)90049-3.

Pourmand, P., Hedenqvist, M.S., Furó, I., Gedde, U.W., 2017. Deterioration of highly filled EPDM rubber by thermal ageing in air: kinetics and non-destructive monitoring. Polym. Test. 64, 267–276. https://doi.org/10.1016/j.polymertesting.2017.10.019.

Rivaton, A., Cambon, S., Gardette, J.L., 2005. Radiochemical ageing of EPDM elastomers. 2. Identification and quantification of chemical changes in EPDM and EPR films γ-irradiated under oxygen atmosphere. Nucl. Instrum. Methods Phys. Res. Sect. B Beam Interact. Mater. Atoms 227, 343–356. https://doi.org/10.1016/j.nimb.2004.09.008.

Rivlin, R.S., 1948. Large elastic deformations of isotropic materials. Philos. Trans. R. Soc. A Math. Phys. Eng. Sci. 240, 459–490. https://doi.org/10.1098/rsta.1948.0002.

Scheirs, J., Bigger, S.W., Billingham, N.C., 1995. A review of oxygen uptake techniques for measuring polyolefin oxidation. Polym. Test.. https://doi.org/10.1016/0142-9418(94)00022-7.

Shabani, A., 2013. Thermal and Radiochemical Aging of Neat and ATH Filled EPDM: Establishment of Structure/Property Relationships. ENSAM, Paris, France.

Shelton, J.R., 1957. Aging and oxidation of elastomers. Rubber Chem. Technol. 30, 1251–1290. https://doi.org/10.5254/3542760.

Tobolsky, A.V., Metz, D.J., Mesrobian, R.B., 1950. Low temperature autoxidation of hydrocarbons: the phenomenon of maximum rates. J. Am. Chem. Soc. 72, 1942–1952. https://doi.org/10.1021/ja01161a023.

Tomer, N.S., Delor-Jestin, F., Singh, R.P., Lacoste, J., 2007. Cross-linking assessment after accelerated ageing of ethylene propylene diene monomer rubber. Polym. Degrad. Stab. 92, 457–463. https://doi.org/10.1016/j.polymdegradstab.2006.1013.

Treloar, L.R.G., 1971a. Viscoelastic Properties of Polymers. John Wiley, London British polymer journal.

Treloar, L.R.G., 1971b. Rubber elasticity. Contemp. Phys. 12, 33–56. https://doi.org/10.1080/00107517108205104.

Volokh, K., 2016. Mechanics of soft materials. Mech. Soft Mater. https://doi.org/10.1007/978-981-10-1599-1.

Volokh, K.Y., 2017. Loss of ellipticity in elasticity with energy limiters. Eur. J. Mech. A/Solids 63, 36–42. https://doi.org/10.1016/j.euromechsol.2016.10.003.

Volokh, K.Y., 2010. On modeling failure of rubber-like materials. Mech. Res. Commun. 37, 684–689. https://doi.org/10.1016/j.mechrescom.2010.10.006.

Volokh, K.Y., 2007. Hyperelasticity with softening for modeling materials failure. J. Mech. Phys. Solids 55, 2237–2264. https://doi.org/10.1016/j.jmps.2007.02.012.

Volokh, K.Y., 2014. On irreversibility and dissipation in hyperelasticity with softening. J. Appl. Mech 81 (7). 074501-074501-3, doi: 10.1115/4026853.

White, J.R., Shyichuk, A.V., 2007. Macromolecular scission and crosslinking rate changes during polyolefin photo-oxidation. Polym. Degrad. Stab. 92, 1161–1168. https://doi.org/10.1016/j.polymdegradstab.2007.04.011.

Williams, M.L., Landel, R.F., Ferry, J.D., 1955. The temperature dependence of relaxation mechanisms in amorphous polymers and other glass-forming liquids. J. Am. Chem. Soc. 77, 3701–3707. https://doi.org/10.1021/ja01619a008.

Wise, J., Gillen, K.T., Clough, R.L., 1995. An ultrasensitive technique for testing the Arrhenius extrapolation assumption for thermally aged elastomers. Polym. Degrad. Stab. 49, 403–418. https://doi.org/10.1016/0141-3910(95)00137-B.

Woo, C.S., Choi, S.S., Lee, S.B., Kim, H.S., 2010. Useful lifetime prediction of rubber componnents using accelerated testing. IEEE Trans. Reliab. 59, 11–17.

Yeoh, O.H., 1990. Characterization of elastic properties of carbon-black-filled rubber vulcanizates. Rubber Chem. Technol. 63, 792–805. https://doi.org/10.5254/3538289.

Yu, H., Wall, L.A., 1965. Radiolytic stress relaxation of an ethylene-propylene copolymer. J. Phys. Chem. 69, 2072–2078. https://doi.org/10.1021/j100890a044.